

Seismic imaging of the Hussar low frequency seismic data

A.Nassir Saeed*, Gary F. Margrave, David C. Henley, J. Helen Isaac and Laurence R. Lines
ansaeed@ucalgary.ca

Abstract

We have implemented an effective seismic processing flow that meets both AVO compliant and seismic imaging objectives for the Hussar low frequency seismic data. The ground roll and pump-jack noise that poses great challenge in seismic processing of the Hussar low frequency experiments were successfully removed via cascaded radial trace filters, while retaining reflection energy of low frequency down to 3Hz.

The resulting migrated section from the new processing shows significant imaging improvement across the entire section, and particularly in the shallow zone (100-500m) that was not clearly seen in previous processing. The phase coherency of the estimated band signal show good spatial coherency down to 3Hz in the processed stacked section. The resulting common image gathers, (CIGs) have shown good reflectivity signal at the far offset of 3450m (an increment of 57%) compared to the 1980m far offset produced by contracting processing company.

Introduction

Figure (1) shows two common image gathers (CIGs) from the pre-stack Kirchhoff migration of the Hussar low frequency experiments that was processed by a contracted processing company. Note that the residual noise left its signature as a step ladder pattern (indicated by arrows in Figure 1) in the CIG gathers which complicates the interpretation of the seismic section, and questions the noise attenuation techniques used. Furthermore, note also that a maximum offset bin of 1980m in the CIG gather will probably affect the accuracy of inverted elastic attributes from the pre-stack (AVO) seismic inversion.

Seismic data processing of the Hussar seismic data

We have designed an AVO compliant seismic data processing flow which, preserves very low frequency signal down to 3Hz in the seismic reflectors while attenuating different types of seismic noise, improve seismic imaging sections, and push the far offset bin in the CIG gathers to maximum feasible distances where reflectivity signals in the zones of interests can be fairly mapped. The radial trace filtering (Henley, 1999) is a robust method to attack and attenuate ground-roll and pump-jack noise (see Figure 2a) since these noises have characteristics velocity and dip at specific frequency band levels. Figure 2b, shows the results after applying radial filters, where dipping noise events were successfully attenuated, and resulting gathers show better continuity of reflection energy that were masked by refraction and ground-roll noise. As a result, the resulting shot gathers show consistent energy distribution across the gathers, as much energy due to ground-roll and pump-jack noise has been attenuated.

Seismic imaging of the Hussar seismic data

We have performed post-stack and pre-stack migration for the Hussar low frequency data using Kirchhoff and phase-shift migration algorithms. Pre-stack migration preparation includes offset binning, and for pre-stack imaging, tests were conducted for optimal apertures distances, maximum dip, stretch mute and maximum offsets used to constrain the common image gathers resulting from pre-stack migration. Residual migration velocity analyses were also conducted to adjust velocity percentages in spatial and temporal directions of the sections.

Figure 3a shows the section from our Pre-stack Kirchhoff migration, while Figure 3b shows the same section from processing company. Note that the contractor has chosen a different datum elevation, replacement velocity, output bin offset and post migration zero phase deconvolution. Hence, the comparison is made based on overall seismic imaging and resolution. The pre-stack image section of data processed by us shows superior resolutions for events from 500-900ms. The contractor's section show some undulating features, that affect the reflectivity of events above and below the zones of interests (900-1200ms). These anticline-shaped features do not represent a marked geological structure in the survey area and are probably due to overestimated velocity values and statics at these specific locations. Figure 4 shows sections of both post-stack and pre-stack phase-shift migration processed for this report. Both show excellent stacked sections, and more details and better seismic resolutions are achieved in the pre-stack phase shift migration compared to the post-stack phase-shift migration. The phase-coherency (Figure 5), which is a measure of spatial coherence of seismic signal shows strong phase coherence signal down to 5Hz, and in many areas along the section it shows good coherency down to 2Hz.

Conclusions

The pre-stack image sections produced from the seismic processing flow applied in this study show superiority in terms of seismic resolution and reflectivity continuity compared to the pre-stack image sections from a seismic processing contractor. Furthermore, we were able to extend the far offset in the CIG gather to 3450m, an increment 57% from the 1980 m far offset of the processing contractor, and resulting common image gathers are free from the step-ladder shape of residual noise that were evident at the CIG gathers produced by the processing contractor. The processed seismic data preserved reflectivity down to 3Hz. Noise attenuation via radial filtering was able to successfully attenuate ground-roll and other seismic noise, while maintain reflectivity at very low frequencies.

Acknowledgements

We thank the CREWES sponsors for financial support of this study. We also gratefully acknowledge support from NSERC .

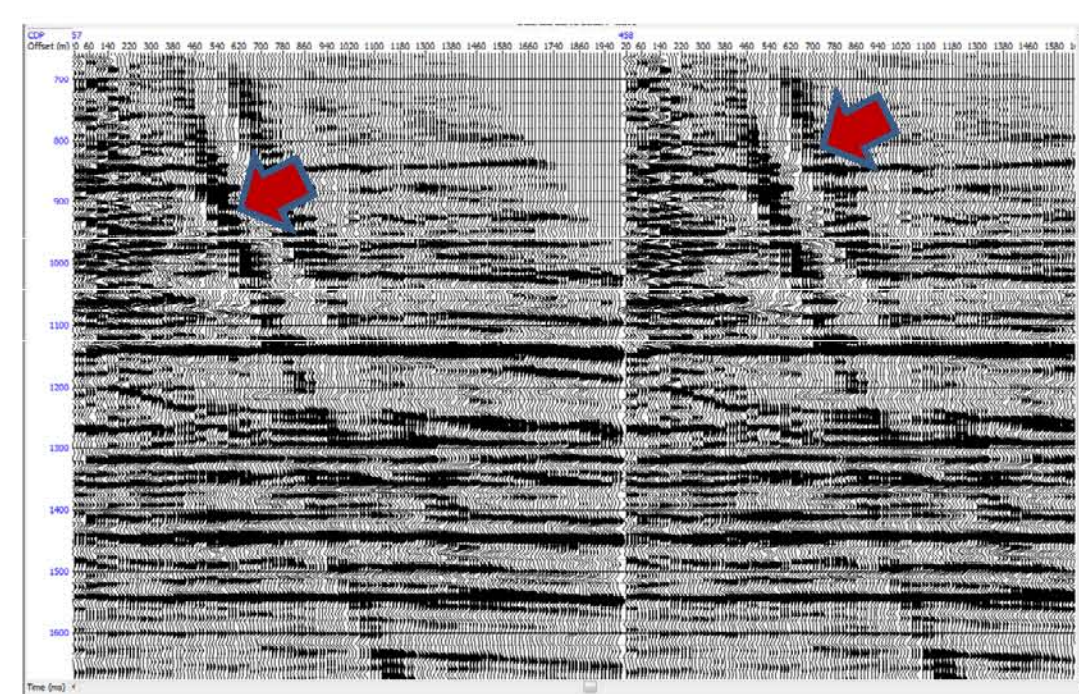


FIG.1. CIG gathers from contracted processing company.

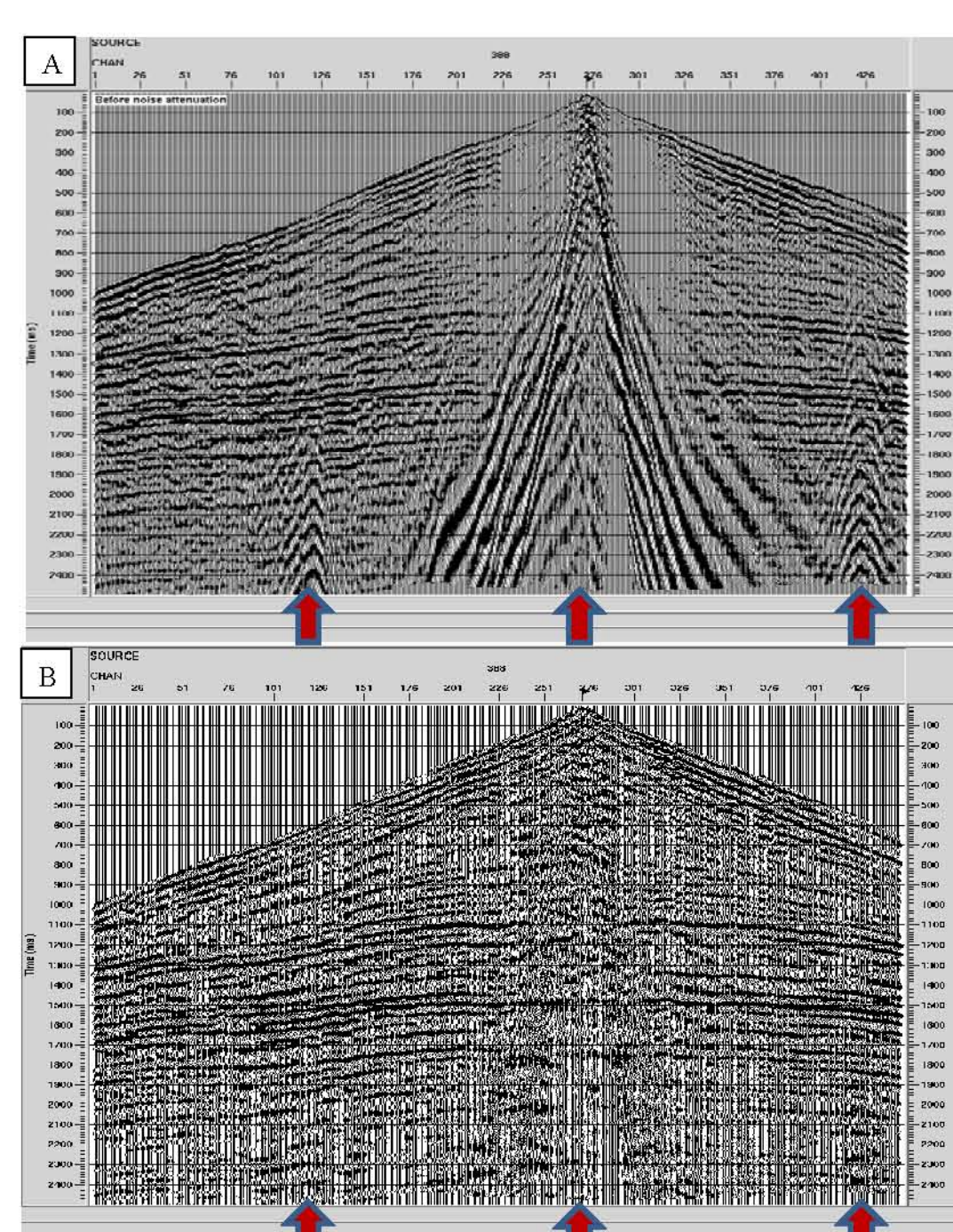


FIG.2. Shot gather before (a) and after (b) noise attenuation via radial filtering.

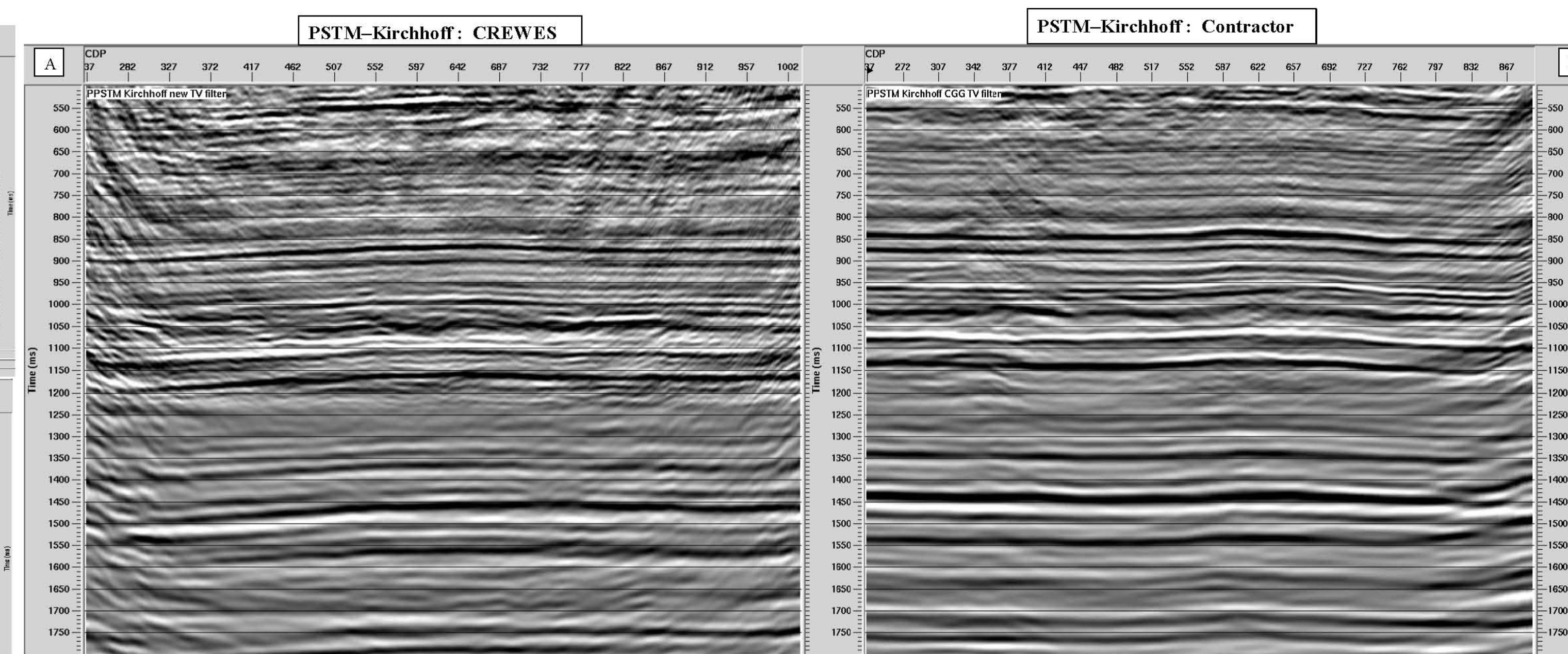


FIG.3. Pre-stack Kirchhoff migrated stack section. (A) Processed in this report. (B) Processed by contracting geophysical processing company.

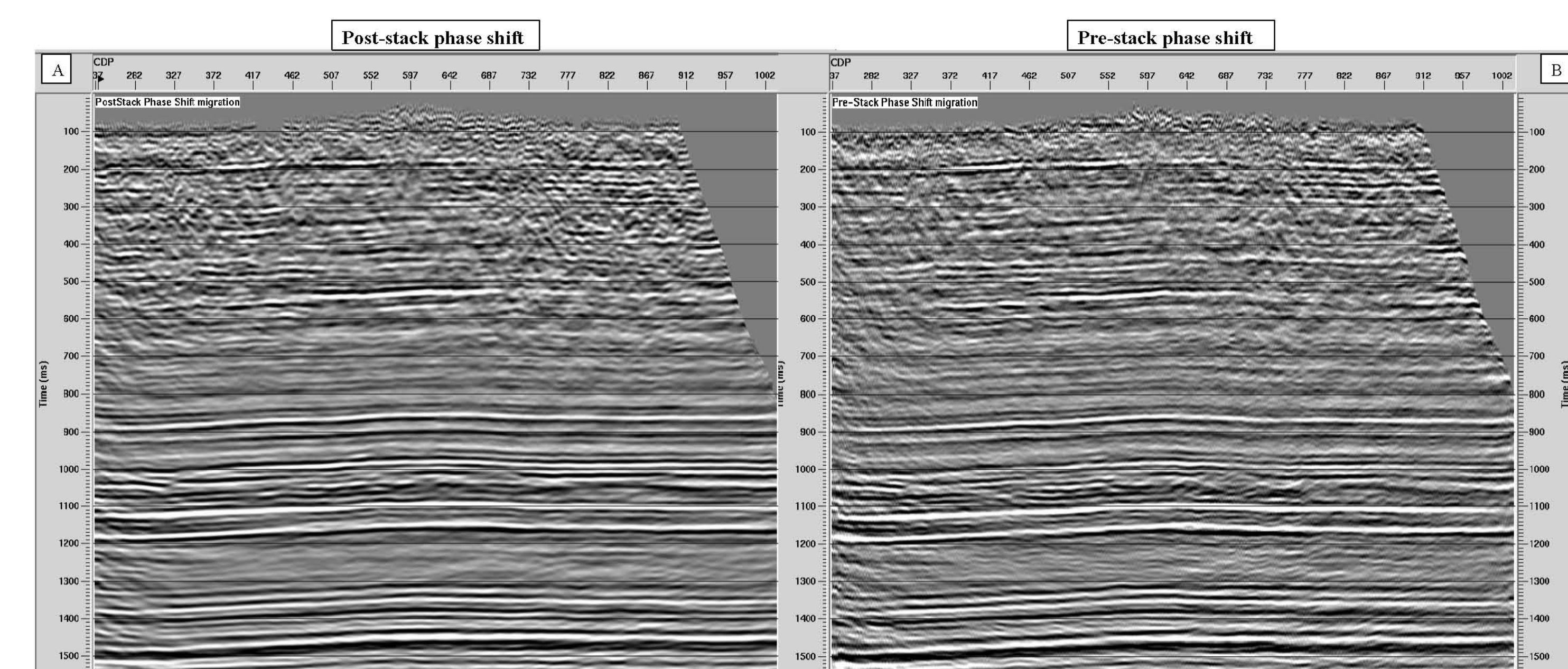


FIG.4. (A) Post-stack phase shift migrated section. (B) Pre-stack phase shift migrated section.

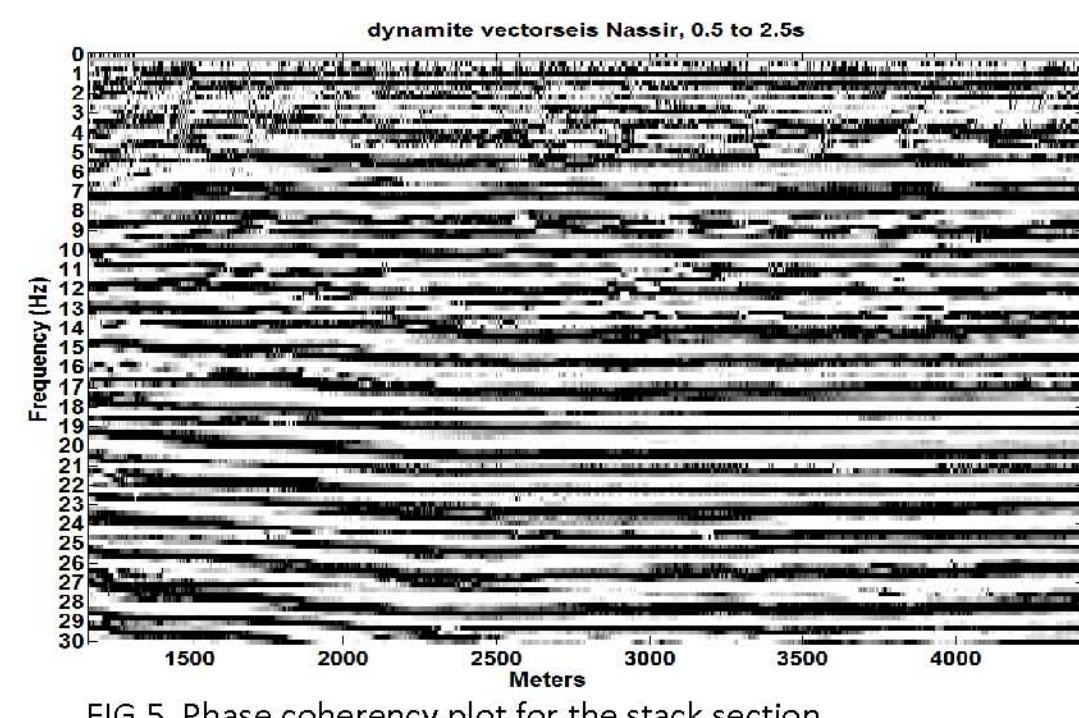


FIG.5. Phase coherency plot for the stack section.